In Situ Studies of the Primary Immune Response to (4-Hydroxy-3-Nitrophenyl)Acetyl. V. Affinity Maturation Develops in Two Stages of Clonal Selection

By Yoshimasa Takahashi, Pinaki R. Dutta, Douglas M. Cerasoli, and Garnett Kelsoe

From the Department of Microbiology and Immunology, University of Maryland School of Medicine, Baltimore, Maryland 21201

Summary

To examine the role of germinal centers (GCs) in the generation and selection of high affinity antibody-forming cells (AFCs), we have analyzed the average affinity of (4-hydroxy-3-nitrophenyl)acetyl (NP)-specific AFCs and serum antibodies both during and after the GC phase of the immune response. In addition, the genetics of NP-binding AFCs were followed to monitor the generation and selection of high affinity AFCs at the clonal level. NP-binding AFCs gradually accumulate in bone marrow (BM) after immunization and BM becomes the predominant locale of specific AFCs in the late primary response. Although the average affinity of NP-specific BM AFCs rapidly increased while GCs were present (GC phase), the affinity of both BM AFCs and serum antibodies continued to increase even after GCs waned (post-GC phase). Affinity maturation in the post-GC phase was also reflected in a shift in the distribution of somatic mutations as well as in the CDR3 sequences of BM AFC antibody heavy chain genes. Disruption of GCs by injection of antibody specific for CD154 (CD40 ligand) decreased the average affinity of subsequent BM AFCs, suggesting that GCs generate the precursors of high affinity BM AFCs; inhibition of CD154-dependent cellular interactions after the GC reaction was complete had no effect on high affinity BM AFCs. Interestingly, limited affinity maturation in the BM AFC compartment still occurs during the late primary response even after treatment with anti-CD154 antibody. Thus, GCs are necessary for the generation of high affinity AFC precursors but are not the only sites for the affinity-driven clonal selection responsible for the maturation of humoral immune responses.

Early in the course of infection, protection is achieved more effectively by preexisting neutralizing serum antibodies than by the later set of antibodies secreted upon restimulation of memory B cells (1). After infection or vaccination, neutralizing serum antibodies can be detected in humans for several decades (2, 3); immunized mice maintain neutralizing antibodies for more than one year. Particularly in situations of rapid and severe pathogenesis, these long-lasting antibodies can provide a powerful mechanism for protection against infection, morbidity, and mortality (1).

One of the characteristics of long-lasting serum antibody is a progressive increase in affinity for the immunogen over time, through a process called affinity maturation (4, 5). After the introduction of hybridoma technology, it was revealed that affinity maturation of serum antibody is achieved by two key events: the generation of antibody variants by V(D)J hypermutation and the subsequent selection of those variants that have high affinity for antigen (6, 7). Over time, these events lead to the preferential accumulation of antibody-forming cells (AFCs)[1] that secrete antibodies with higher affinities and faster on-rates (8–10). It is widely believed that inter- and intraclonal competition for the antigen retained on the follicular dendritic cells of germinal centers (GCs; 11–13) is the basic mechanism that promotes the selective accumulation of high affinity memory B cells and AFCs over time (5). However, little is known about the cellular and molecular mechanisms underlying this selection.

After immunization with T cell–dependent antigens, antigen-responsive B cells in the spleen accumulate and proliferate in the margins of the T cell zones, or the periarteriolar lymphoid sheaths (PALS), and enter into two developmental pathways. B cells can either remain to form foci of AFCs

[1]*Abbreviations used in this paper:* 7-AAD, 7-aminoactinomycin D; AFC, antibody-forming cell; BM, bone marrow; CG, chicken-γ-globulin; ELISPOT, enzyme-linked immunospot; GC, germinal center; HRP, horseradish peroxidase; K_a, association constant; NP, (4-hydroxy-3-nitrophenyl) acetyl.

at the margin of the PALS, or can return to the lymphoid follicle to establish GCs (14–16). The early foci of AFCs mainly produce low affinity antibodies encoded by germline genes (17, 18). These AFCs peak in number at days 8–10 after immunization and then rapidly decline to basal levels (16, 19). Concomitantly, AFCs in the bone marrow (BM) start to appear around day 10 and gradually accumulate during the late primary response (19–21). As a result, a few months after immunization the great majority of antigen-specific AFCs are present in BM. Since serum antibodies have relatively short half-lives (22), it is now accepted that the long-lived BM AFCs are responsible for long-lasting serum antibody titers (23). Thus, cellular events leading to the preferential accumulation of high affinity AFCs in BM are key elements in the affinity maturation of serum antibody and are crucial for protective immunity.

The GC has been identified as a site for the generation of high affinity antibody variants through antigen-driven V(D)J hypermutation and clonal selection (24–27). Lymphocytes in the GC regain many characteristics of those present in primary lymphoid tissues (28–32), including high sensitivity to antigen receptor–mediated death (28–31), consistent with the idea that GCs are specialized sites for clonal selection. Previous reports also suggest that BM AFCs are derived from GC B cells (33–35), implying that GCs are sites for the generation and selection of high affinity BM AFCs. However, it remains unclear to what extent mutation and selection occur exclusively in GCs (36, 37). Recently, Smith et al. (35) showed that high affinity B cells migrate into the BM to become AFCs during the primary GC reaction and concluded that the frequency of high affinity AFCs in BM quickly plateaus. These results suggest that the GC alone is necessary and sufficient for the generation of high affinity BM AFCs. In seeming contradiction to these findings, the affinity maturation of serum antibody is known to develop slowly during the first 3 wk after immunization; indeed, the majority of affinity maturation in serum antibody takes place after day 30 of the primary response (38). Thus, it remains possible that affinity-driven selection takes place in the post-GC environment. This notion is also compatible with the previous observations that clonal selection in each GC takes place independently (17) and that low affinity B cells can survive the selection process within GCs lacking high-affinity competitor B cells (Dal Porto, J.M., A.M. Haberman, D.M. Cerasoli, M.J. Shlomchik, and G. Kelsoe, manuscript submitted for publication)[2] and move into the memory B cell pool (35).

To understand better the mechanisms of affinity maturation of serum antibody, we have used the clonally restricted antibody response of C57BL/6 mice to the (4-hydroxy-3-nitrophenyl)acetyl (NP) hapten (39–42) to investigate the role of GCs in the generation and selection of long-lived, high affinity AFCs in BM. Here, we show that the generation of high-affinity precursors of BM AFCs by somatic mutation is totally dependent on the GC reaction, since the frequency of H chain V(D)J mutations present in BM AFCs increased only while GCs were present in the spleen, and the appearance of high affinity BM AFCs could be blocked significantly by the disruption of GCs with anti-CD154 (CD40 ligand) antibody. However, the subsequent selection for higher affinity AFCs does not require GCs, and affinity-based selection among BM AFCs continues long after the end of the GC reaction.

Materials and Methods

Antigens and Antibodies. Succinic anhydride esters of NP were reacted with chicken-γ-globulin (CG; Sigma Chemical Co., St. Louis, MO) or BSA (U.S. Biochemical Corp., Cleveland, OH) as previously described (16). The coupling ratio of each conjugate was determined spectrophotometrically. Normal hamster IgG was purchased from Pierce Chemical Co. (Rockford, IL). Monoclonal antibodies specific for mouse CD154 (MR1), IgM^b (AF6-78), and λ1 L chain (Ls136) were purified over protein G–Sepharose (Pharmacia Biotech AB, Uppsala, Sweden) from culture supernatants of each hybridoma. Horseradish peroxidase (HRP)–conjugated goat anti–mouse IgG_1 and alkaline phosphatase–conjugated anti–mouse IgM antibodies were purchased from Southern Biotechnologies, Associates (Birmingham, AL). Anti-FcγRI/RII (2.4G2), FITC-labeled GL-7, PE-conjugated anti-B220, biotinylated anti–Mac-1, biotinylated anti–Gr-1, biotinylated anti-Thy1.2, and PE-conjugated anti-CD138 (syndecan) antibodies were purchased from PharMingen (San Diego, CA).

Immunizations. C57BL/6 mice were immunized intraperitoneally with 50 μg of NP_{20}–CG conjugate precipitated in alum. Anti-CD154 antibody or normal hamster IgG was administered intravenously on days 6, 8, and 10, days 10, 12, and 14, or days 16, 18, and 20 after primary immunization, with 300 μg of antibody per each injection.

Enzyme-linked Immunospot. The frequency of NP-specific AFCs from both splenocytes and BM cells was estimated by enzyme-linked immunospot (ELISPOT) using two different coupling ratios of NP–BSA. Nitrocellulose filters were coated with 50 μg/ml NP_5–BSA, NP_{26}–BSA, or BSA in PBS at 4°C overnight, and then blocked with 1% BSA in PBS. Splenocytes (10^5 cells/well) or BM cells (5×10^5 cells/well) were incubated on the nitrocellulose filters in 96-well plates at 37°C, 5% CO_2. After a 2-h incubation, nitrocellulose filters were washed with PBS containing 50 mM EDTA once, followed by PBS containing 0.1% Tween 20 (Sigma Chemical Co.) twice and PBS once. Filters were double-stained with alkaline phosphatase–conjugated anti-IgM and HRP-conjugated anti-IgG_1 antibodies. Alkaline phosphatase and HRP activities were visualized using 3-aminoethyl carbozole and napthol AS-MX phosphate/fast blue BB (Sigma Chemical Co.), respectively, as previously described (16). The frequency of high affinity and total AFCs was determined from NP_5–BSA– and NP_{26}–BSA–coated filters after background on BSA-coated filters was subtracted.

Several J558L myeloma lines (H^-; $\lambda1^+$) transfected with an Igγ1 expression vector carrying different VDJ rearrangements derived from NP-binding B cells[2] were incubated at 100 cells/well on nitrocellulose filters coated with these NP–BSA conjugates to determine the threshold of antibody affinity which can be detected by each NP–BSA conjugate. Transfectomas secreting NP-binding antibody with an association constant (K_a) = 2.0×10^7

[2] Dal Porto, J.M., A.M. Haberman, M.J. Schlomchik, and G. Kelsoe, manuscript submitted for publication.

M^{-1} (H33Lγ1/λ1) could be detected by both NP_5–BSA and NP_{26}–BSA. However, transfectomas with a $K_a = 10^6\ M^{-1}$ could be detected by NP_{26}–BSA, but not by NP_5–BSA. Transfectomas with a $K_a = 2.3 \times 10^5\ M^{-1}$ could not be detected by either NP–BSA coat. Thus, AFCs secreting antibody with a $K_a \geq 2.0 \times 10^7\ M^{-1}$ can be detected with NP_5–BSA, and those with a $K_a \geq 10^6\ M^{-1}$ can be detected with NP_{26}–BSA.

Measurement of Serum IgG$_1$ or λ1 Antibody. IgG_1 or λ1 antibody specific for the NP hapten was detected by ELISA using two different coupling ratios of NP–BSA as the coating antigens. In brief, 96-well flat bottom plates (Falcon; Becton Dickinson, Oxnard, CA) were coated with 50 μg/ml NP_5–BSA or NP_{26}–BSA in 0.1 M carbonate buffer (pH 9.0) at 4°C overnight, and blocked with 0.5% BSA in carbonate buffer. Serially diluted sera were then added to each well and incubated at 4°C overnight. On each plate, serially diluted H33Lγ1/λ1, a monoclonal antibody recognizing the NP hapten ($K_a = 2.0 \times 10^7\ M^{-1}$)[2] was also included as a control. After washing with PBS containing 0.1% Tween 20, HRP-conjugated goat anti–mouse IgG_1 or biotinylated Ls136 was added and incubated at room temperature for 2 h. HRP-conjugated streptavidin was added to detect biotinylated Ls136; HRP activity was visualized using a TMB peroxidase substrate kit (Bio-Rad Laboratories, Hercules, CA) and optical densities were determined at 450 nm. The concentrations of anti-NP IgG_1 or λ1 antibodies were estimated by comparison to standard curves created from the H33Lγ1/λ1 control on each plate. To estimate the affinity of NP-binding antibody in the sera, the ratio of NP_5-binding antibody to NP_{26}-binding antibody was calculated (43).

The affinity threshold of antibody binding to each NP–BSA conjugate was determined by using several monoclonal antibodies with different affinities for NP. H33Lγ1/λ1 bound equally well to both NP–BSA conjugates, whereas a monoclonal antibody with a $K_a = 10^6\ M^{-1}$ showed a 20-fold lower binding to NP_5–BSA than to NP_{26}–BSA. A monoclonal antibody with a $K_a = 2.3 \times 10^5\ M^{-1}$ had a 10-fold lower binding to NP_{26}–BSA than one with a $K_a = 1.0 \times 10^6\ M^{-1}$. Thus, antibody with a $K_a \geq 2.0 \times 10^7\ M^{-1}$ can be detected with NP_5–BSA, and one with a $K_a \geq 10^6\ M^{-1}$ can be detected with NP_{26}–BSA.

Flow Cytometry. Single cell suspensions of splenocytes and BM cells were prepared and RBCs were depleted by incubation in 0.83% NH_4Cl; cells were then washed with PBS (pH 7.4) containing 2% FCS and 0.08% sodium azide at 4°C for cytometric analysis, or washed with deficient RPMI 1640 (Irvine Scientific, Santa Ana, CA) containing 2% FCS for sorting. To estimate the prevalence of GC B cells, cells were stained with FITC-labeled GL-7, PE-conjugated anti-B220, and 7-aminoactinomycin D (7-AAD; Molecular Probes, Inc., Eugene, OR) for 30 min after incubation with anti-FcγRI/RII for 10 min to block FcγR-mediated binding. After washing three times, >30,000 events were collected on a FACSort® machine (Becton Dickinson, Mountain View, CA) and the percentage of GL-7^+, $B220^+$ cells were calculated from live lymphocytes selected by forward-side scatter pattern and exclusion of 7-AAD, using CellQuest software (version 3.01; Becton Dickinson).

To collect BM AFCs, BM cells pooled from four or five mice were blocked with anti-FcγRI/RII and then stained with biotinylated anti-IgM^b, –Mac-1, –Gr-1, and –Thy1.2 antibodies for 30 min. After three washes, cells were incubated with streptavidin-conjugated microbeads (Miltenyi Biotec, Gladbach, Germany) for 15 min. Cells attached to microbeads were depleted by passage through a CS column (Miltenyi Biotec) in a magnetic field based on the manufacturer's protocol. Recovered cells were stained with FITC-labeled Ls136, PE-conjugated anti-CD138, Tricolor-conjugated streptavidin (Caltag Laboratories, South San Francisco, CA), and 7-AAD. Finally, $\lambda1^+$, $CD138^+$ cells within the Tricolor$^-$ (IgM^{b-}, Mac-1^-, Gr-1^-, Thy1.2^-), 7-AAD^- fraction (routinely between 0.003 and 0.015% of cells) were sorted into Trizol (GIBCO BRL, Gaithersburg, MD) containing 50 μg/ml tRNA (*Escherichia coli*; Boehringer Mannheim, Indianapolis, IN) at 50–200 cells per tube using a FACStar Plus® (Becton Dickinson). Sorting routinely yielded populations of >90% purity.

Affinity Measurement of Serum Antibody by Fluorescence Quenching. In addition to differential ELISAs, the affinity of anti-NP serum antibody was estimated by fluorescence quenching (44).[2] In brief, serum IgG was purified from cohorts of mice using protein G–Sepharose and adjusted to a concentration of 50 μg/ml in 2 ml of PBS containing 0.02% Tween 20. Titrations were carried out by adding monovalent NP hapten (NP-caproate; Genocys, Woodlands, TX) over a three-log molar range (10^{-8}–10^{-5}). For the correction of nonspecific quenching, quenching from an irrelevant antibody, a mouse anti-dextran IgG_1 (MOPC 21; Sigma Chemical Co.), was also determined.

Sequence Analysis of VDJ DNA from BM AFCs. Total RNA was extracted from sorted, Trizol-solublized BM AFCs based on manufacturer's protocol. First strand cDNA was synthesized from total RNA using a primer complementary to the C_{H1} region of $C_{\gamma1}$ ($C_{\gamma1}$ primer; 5′-GAGTTCCAGGTCACTGTCACTGGCTCAGGGA-3′) and a Superscript Kit (GIBCO BRL). 5 μl of cDNA solution was used as a template for two rounds of nested PCR to amplify V_H genes combined to the $C_{\gamma1}$ region. PCR amplification, cloning, and sequencing of V_H genes were performed as previously described (24, 30), except that the $C_{\gamma1}$ primer was used as an antisense primer for the first round of PCR amplification. This PCR scheme minimizes any contribution of VDJ rearrangements from immature BM B cells to the data set.

Results

Primary Immunization with NP–CG Induces Long-lasting Serum Antibody and High Frequencies of Specific AFCs in BM. After primary immunization with 50 μg of NP–CG, the number of splenic AFCs secreting NP-specific, IgG_1 antibody peaked at day 8 after immunization and then rapidly declined (Fig. 1 *A*). Concomitantly, the number of BM AFCs slowly grew, such that by 4 mo after immunization the frequency of hapten-specific AFCs in the BM was >10-fold higher than in the spleen. The increased frequency and persistence of NP-specific AFCs in the BM correlated with persistent titers of NP-binding IgG_1 antibody in the serum (Fig. 1 *B*). Maximum levels of circulating antibody (900–1700 μg/ml) were observed at day 12 after immunization. Circulating antibody concentrations then declined to ~50% of this peak and remained stable from day 32 to day 119 after immunization. Combined with the relatively short half-life of circulating antibody (22) and the prominent role of BM in long-term antibody production (20, 21), persistent IgG_1 serum antibody appears to be the product of BM AFCs.

The near exclusive use of λ1 L chain in NP-binding antibody during the early primary response is diminished in secondary responses which support increased percentages of κ-bearing, NP-specific antibody (20–40%; references

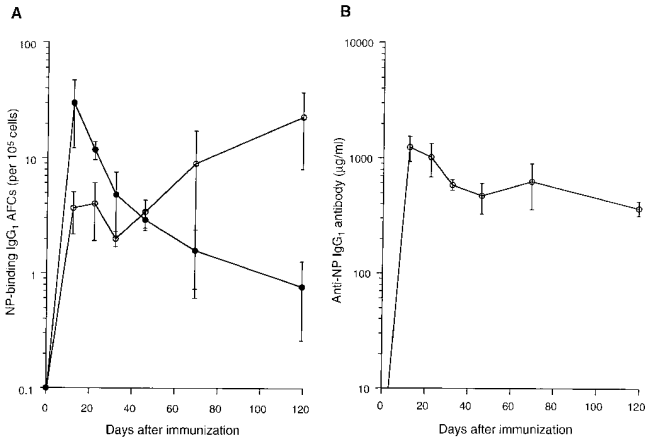

Figure 1. Kinetics of NP-binding IgG_1 AFCs and serum IgG_1 antibody elicited by primary immunization with NP–CG. Numbers of NP-binding AFCs from BM (*open circles*) and spleen (*filled circles*) were determined by ELISPOT using NP_{26}–BSA as the capture antigen (*A*). NP-binding serum antibody was determined by ELISA using NP_{26}–BSA (*B*). The data represent the mean ± SD from three to nine individual mice per time point.

40, 45). To estimate the stability of λ1 expression among persistent IgG_1 antibody, both the λ1 and the IgG_1 antibody titer in each sera was calculated by ELISA using the same control antibody bearing IgG_1/λ1. As shown in Table 1, the percentage of λ1/IgG_1 remained above 80% from day 46 to day 119 after immunization. Thus, no significant replacement by NP-specific antibody-bearing κ L chain was observed.

Kinetics of the Primary GC Response. To quantitate the GC reaction over the course of a primary humoral response, we determined the frequency of splenic GL-7^+ $B220^+$ GC B cells by flow cytometry (32) at days 12, 22, 32, 46, and 69 after immunization with NP–CG (Fig. 2). Confirming our histologic determinations (16), GC B cells increased from background levels of 0.4 ± 0.3% (average ± SD) to a peak of 2.3 ± 0.6% at day 12 after immunization. Subsequently, the GC reaction quickly waned; at day 22 of the response the frequency of GC B cells fell to 1.1 ± 0.4%, reaching naive levels by day 32. Thus, the primary antibody response (Fig. 1) continues long after the GC reaction can no longer be detected (Fig. 2).

The Average Affinity of BM AFCs and Serum Antibody Increases after GCs become Undetectable. The average affinity of AFCs from both spleen and BM was estimated by calculating the ratios of AFCs enumerated on ELISPOT substrates with sparse (high affinity AFC) or abundant (low and high affinity AFC) levels of NP hapten (Fig. 3). This assay was validated with cells secreting NP-specific monoclonal antibodies with different affinities for NP (data not shown). To be detected on the NP_5–BSA substrate, AFC had to secrete antibody with a $K_a \geq 2.0 \times 10^7\ M^{-1}$; AFC secreting antibody with 20-fold lower affinity could be detected only on NP_{26}–BSA. The ratio of high affinity versus total NP-binding AFCs in BM rapidly increased from 29.2% to 51.5% while GC B cells were present in the

Table 1. *Continued Predominance of λ1$^+$ Antibody in the Primary Anti-NP Response*

Days after immunization	NP-binding primary antibody		
	Average concentration μg/ml		Percent λ1$^+$ (average ± SD)
	λ1$^+$	γ1$^+$	
22 (n = 4)	1,249	1,082	116 ± 5
32 (n = 5)	753	637	120 ± 18
46 (n = 4)	513	581	90 ± 13
69 (n = 6)	296	369	82 ± 9
119 (n = 4)	395	467	91 ± 12

spleen (Fig. 2), and later continued a more gradual, but appreciable increase (68.4% at day 32, 85.4% at day 119; $P < 0.05$, Student's t test) after the GC response became undetectable. The average affinity of NP-binding serum antibody was also determined in the same mice by ELISA (Fig. 4 *A*) and fluorescence quenching (Fig. 4 *B*). Mirroring affinity

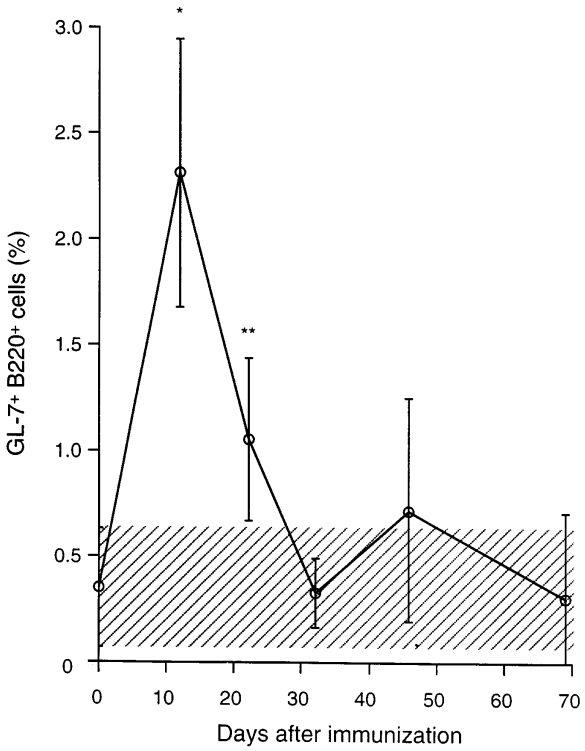

Figure 2. Kinetics of the primary GC response. The percentage of GC B cells out of live lymphocytes was assessed by co-staining with anti-B220 and GL-7 antibodies. The data represent the average number and standard deviation from individual mice (n = 3–9). The background staining with these antibodies was determined from naive mice, and is indicated (along with SD) by the hatched area. *, **: Staining that is statistically different from background at $P < 0.001$ and $P < 0.005$, respectively, using the student's t test.

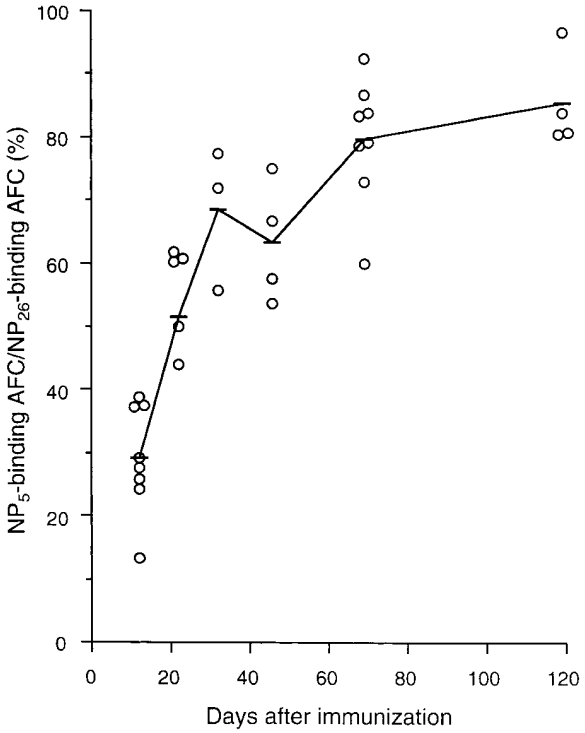

Figure 3. The average affinity of NP-binding IgG_1 BM AFCs increases after GCs become undetectable. The frequency of NP_5-binding and NP_{26}-binding IgG_1 AFCs from BM was determined by ELISPOT. The ratios of NP_5-binding versus NP_{26}-binding AFCs were then plotted as shown. Each point represents an individual mouse.

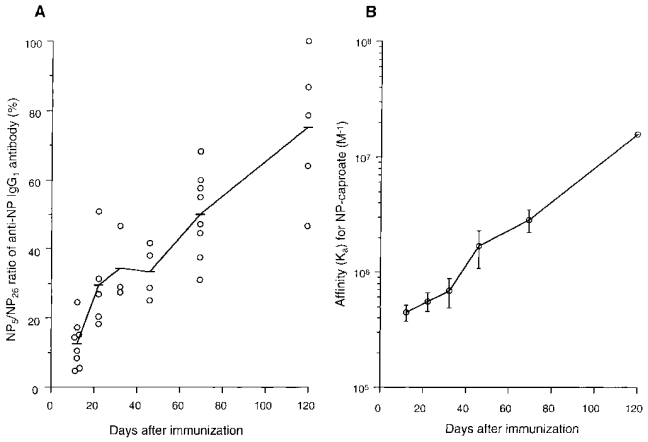

Figure 4. The average affinity of NP-binding IgG_1 antibody in the serum continues to increase after GCs become undetectable. The average affinity of serum antibodies at different time points was estimated by ELISA (*A*) and fluorescence quenching (*B*). (*A*) The concentrations of NP_5-binding and NP_{26}-binding IgG_1 antibody were determined by ELISA and the ratios of NP_5 versus NP_{26}-binding IgG_1 antibody were plotted. Each dot represents the result from an individual mouse. (*B*) The K_a of IgG serum antibody against a monovalent form of NP hapten was determined by fluorescence quenching. Sera was pooled from two to four mice of each group and IgG antibody was purified by passing through a protein G–Sepharose column. The data represent the mean ± SD from two independent serum pools.

increases in BM AFCs, the average affinity of serum antibody also increased from day 12 to day 119 of the response (Fig. 4). Indeed, the majority of affinity maturation in the serum antibody took place after day 32, when GC B cells could no longer be detected in the spleen. The different pattern of increase in affinity between BM AFCs and serum antibody (Figs. 3 and 4) is likely to be due to the rate of decay (half-life) of serum IgG_1 antibody. Together, these data suggest that antigen-driven clonal selection for high affinity BM AFCs or their precursors continues in the post GC environment.

Affinity Maturation of Serum Antibody Is Reflected in the Somatic Genetics of the BM AFC Population. Initially, NP–CG activates a diverse population of splenic B cells that bear the λ1 L chain (39, 40) and H chain genes containing members of the V186.2 and V3 subfamilies of J558 V_H gene segments C1H4, V23, CH10, V186.2, 24.8, or 165.1 (46, 47). With time, interclonal competition (47)[2] leads to the predominance of higher affinity cells carrying V186.2-to-DFL16.1 rearrangements with a tyrosine-rich junctional motif, YYGS (42, 48) and an affinity-enhancing W→L mutation at position 33 (35, 49, 50).

To follow clonal competition and selection in BM AFCs, we enriched this population by depleting IgM^+, $Gr\text{-}1^+$, $Mac\text{-}1^+$, and $Thy1.2^+$ cells from BM and we then purified $\lambda1^+$, $CD138^+$ cells by fluorescence-activated cell sorting. Typically, >40% of this population secreted NP-binding, IgG_1 antibody by ELISPOT. Enriched BM AFC populations obtained at days 12, 46, and 119 after immunization were subjected to a reverse transcriptase PCR that preferentially amplifies cDNA representing rearrangements of the V186.2 and V3 subfamilies of J558 V_H gene segments joined to Cγ1. Cloned VDJ segments from each time point (*n*: day 12 = 18; day 46 = 31; day 119 = 22) were then sequenced to follow the somatic genetics of the BM AFC population over the course of the primary response.

Table 2 summarizes these data and shows that clonal dominance by IgG_1 B cells expressing V186.2-to-DFL16.1 rearrangements takes place in the BM, albeit at a slower pace than reported for the splenic compartment. At day 12, some 78% of the VDJ rearrangements amplified from sorted $\lambda1^+$ BM AFCs contained the V186.2 gene segment; fewer than half of these (43%) were rearranged to DFL16.1 and none contained the YYGS motif in CDR3. However, with time the frequency of canonical V186.2 rearrangements increased; by day 119 only V186.2 rearrangements were recovered and the great majority of these (91%) were fused to DFL16.1. Almost half (41%) of the VDJ fragments from day 119 BM AFCs encoded YYGS at the V-to-D junction (Table 2).

Mutations in transcribed VDJ rearrangements accumulated in BM AFCs, reaching a maximum average of 4.6 mutations per V_H gene segment by day 119 after immunization (Table 2). The apparent increase in V_H mutations was most rapid in the earliest phase of the response. Indeed, the rate of accumulated mutations in the first 12 d of the

Table 2. *Somatic Genetics of λ1⁺ AFC in BM of C57BL/6 Mice Immunized with NP–CG*

	d12	d46	d119
V186.2 (%)	78	90	100
Other (%)	22	10	0
V186.2 mutation frequency	2.0 (n = 14)	3.4 (n = 28)	4.6 (n = 22)
R/S ratio			
CDR1 (14.0/1)*	>1.0/1	1.2/1	>9.0/1
CDR2 (4.3/1)	>4.0/1	10.0/1	3.8/1
FW (3.1/1)	2.3/1	2.1/1	2.6/1
DFL16.1 (%)‡	43	79	91
YYGS (%)§	0	25	41
W→L 33 (%)‖	0	25	23

All sequence data are available from EmBL/GenBank/DDBJ under accession number AF028612-25 (day 12), AF028626-53 (day 46), and AF028654-75 (day 119).

*Expected R/S ratio of V_HV186.2 given random mutagenesis.

‡The percentage of rearrangements using DLF16.1 gene segments in all rearrangements of V_HV186.2.

§The percentage of rearrangements encoding YYGS in CDR3 in all rearrangements of V_HV186.2.

‖The percentage of all V_HV186.2 rearrangements bearing a W→L mutation in 33.

response is 11-fold greater than that observed late (days 47–119) in the response (0.17 versus 0.016 V_H mutations per day). The frequency of silent mutations present in BM AFCs did not increase after day 46. Together, these observations suggest that most, if not all, V_H mutations present in mature populations of IgG_1 BM AFCs were introduced during the first 30 d of the response.

The changing distribution and frequency of specific V_H mutations in BM AFCs, like the eventual dominance of canonical VDJ rearrangements, suggests affinity-driven selection in the BM compartment. On average, the ratio of replacement/silent mutations was suppressed in the framework regions of mutated V_H genes. More significantly, the frequency of W→L mutations in codon 33 increased from 0% at day 12 after immunization to a maximum of 25% by day 46 (Table 2).

Disruption of GCs Selectively Inhibits the Appearance of High Affinity BM AFCs and Impairs Affinity Maturation of Serum Antibody. To elucidate the role of the GC reaction in the production of high affinity BM AFCs, we created GC-deficient mice by injecting them with the anti-CD154 (CD40 ligand) monoclonal antibody, MR1 (51). MR1-treatment after initiation of primary anti-NP responses results in complete disruption of nascent GCs without inhibiting the splenic foci of AFCs or early serum antibody titers (30, 52). Previous histological studies (16) and Fig. 2 demonstrate that splenic GCs appear by day 4–6 after immunization and reach peak cell numbers per volume by day 12–16. The primary GC reaction then declines to basal levels by day 32 after immunization (53) (Fig. 2). In this study, administration of MR1 antibody was conducted on three different schedules: days 6, 8, and 10 (early schedule), which permitted GCs to be formed but permitted little or no clonal selection; days 10, 12, and 14 (intermediate schedule), which allowed GCs to support the initiation of V(D)J hypermutation and selection; and days 16, 18, and 20 (late schedule), which was permissive for extensive mutation and selection. 2 d after the final MR1 treatment, histological staining of spleen sections with peanut agglutinin and enumeration of GL-7⁺ B220⁺ splenocytes by flow cytometry were performed to confirm that splenic GCs were no longer present. In all experiments, administration of MR1 antibody resulted in the complete loss of splenic GC

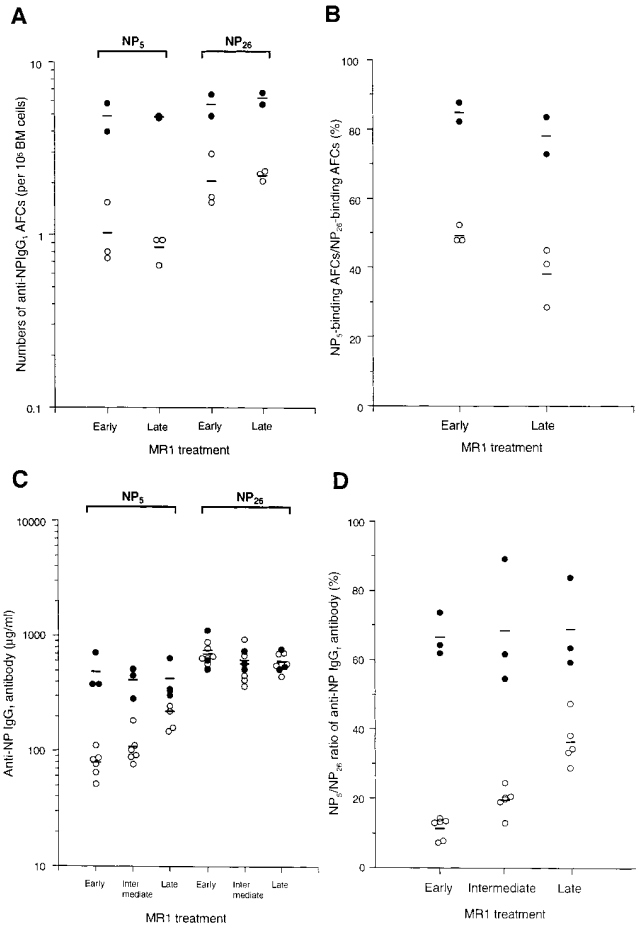

Figure 5. Disruption of GCs impairs affinity maturation of serum antibody due to the selective inhibition of high affinity BM AFCs. MR1 (*open circles*) or control antibody (*filled circles*) was intravenously administered at days 6, 8, and 10 (early), days 10, 12, and 14 (intermediate), or days 16, 18, and 20 (late). At day 69 after immunization, sera and BM cells were recovered. Numbers of NP_5-binding and NP_{26}-binding AFCs in BM were determined by ELISPOT (*A*) and the ratios of NP_5-binding versus NP_{26}-binding AFCs were plotted (*B*). The amount of NP_5-binding or NP_{26}-binding IgG_1 antibody in each serum was determined by ELISA (*C*) and the ratios of NP_5-binding versus NP_{26}-binding antibody were plotted (*D*).

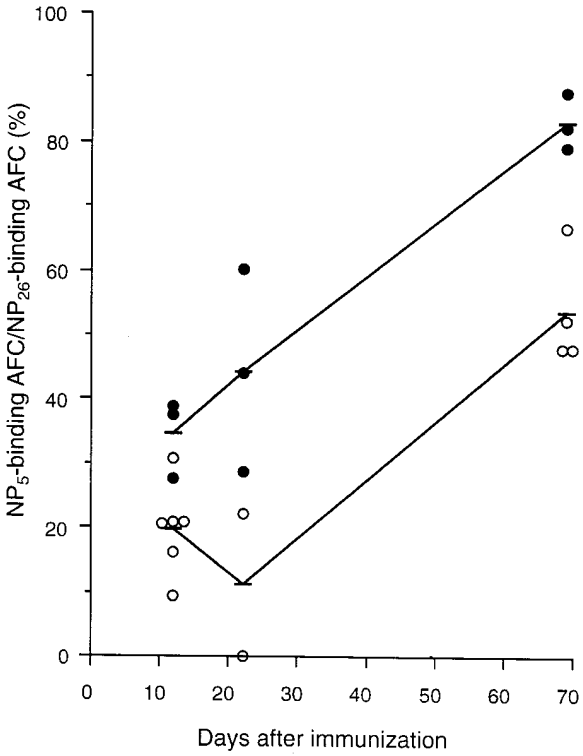

Figure 6. Disruption of GCs does not impair the process of affinity-driven selection of BM AFCs. Mice were injected with NP-CG and given MR1 antibody (*open circles*) or control Ig (*filled circles*) 6, 8, and 10 d later. NP_5- and NP_{26}-binding, IgG_1 AFCs in the BM of both groups were enumerated by ELISPOT assay on days 12, 22, and 69 of the response. Ratios of NP_5- to NP_{26}-binding AFCs were plotted; each point represents a single mouse.

structures and reduction of GL-7^+ $B220^+$ cell numbers to background levels (data not shown). Mice treated with a control hamster antibody showed no significant changes in GC structure or cell numbers relative to untreated mice (data not shown). The numbers of high affinity and total NP-binding AFCs in the BM of MR1-treated mice were determined at day 69 after immunization (Fig. 5). Injection of MR1 antibody selectively inhibited the emergence of high affinity BM AFCs (Fig. 5 *A*) and led to decreased ratios of high affinity versus total NP-binding AFCs (Fig. 5 *B*). The MR1 antibody, but not hamster Ig, also inhibited the production of high affinity serum antibody for NP without suppressing the titers of lower affinity antibody (Fig. 5 *C*). Inhibition of high affinity antibody was most effective when MR1 was given on the early schedule; prolonging the GC reaction by delaying the injection of MR1 allowed proportionate recovery of the high affinity serum antibody (Fig. 5 *D*), and MR1-treatment after the GC reaction was complete (days 46, 48, and 50) had no effect on either high affinity BM AFCs or on serum antibody (see below). Thus, the average affinity of serum antibody for NP in immunized mice receiving the early schedule of passive MR1 antibody was about five times lower ($K_a = 6.1 \times 10^5\ M^{-1}$) than antibody from control mice ($K_a = 2.9 \times 10^6\ M^{-1}$). These data suggest that the major, if not sole, source of high affinity cells in the BM AFC compartment is the GC reaction. Lower affinity AFCs may represent GC emigrants that have not yet achieved high affinity by mutation and/or selection.

Disruption of GCs Does Not Impair Affinity-driven Selection of BM AFCs. Disruption of nascent GCs by the administration of MR1 antibody at days 6, 8, and 10 after immunization suppresses the high affinity compartment of BM AFCs and the affinity maturation of serum antibody (Fig. 5). However, affinity maturation within the small residuum of higher affinity BM AFCs remained intact (Fig. 6). The affinities of BM AFCs were determined on days 12, 22, and 69 after immunization with NP–CG and early MR1 treatment. Consistent with results illustrated in Fig. 5, the frequency of BM AFCs capable of binding NP_5–BSA on days 22 and 69 was suppressed. Nonetheless, the relative fraction of high affinity BM AFCs increased in MR1-treated mice in parallel with control animals. This increase occurred in the complete absence of detectable GCs or GC cells in the spleens of MR1-treated mice. Thus, while the GC reaction limits the extent and quality of the high affinity compartment of BM AFCs, antigen-driven selection in this compartment is independent of GCs.

This late phase of affinity maturation is relatively independent of CD154-mediated costimulation and thus is distinct from the earlier selection in GCs. MR1-treatment over days 46–50 after immunization did not suppress the number ($5.1/10^5$ versus $5.3/10^5$) or fraction of high affinity (81 versus 73%) BM AFCs, nor did it diminish high affinity serum antibody responses (219 μg/ml versus 140 μg/ml).

Discussion

Affinity maturation of serum antibody is a cardinal but poorly understood phenomenon of humoral immune responses to thymus-dependent antigens. Early studies attempted to explain affinity maturation in Darwinian terms: clonal competition for decreasing amounts of antigen selectively maintains proliferation in B cells bearing the most avid receptors (5). More recent work supports this view and demonstrates that clonal competition is coupled to a process of V(D)J hypermutation in GCs (24, 25). It is now widely believed that affinity maturation is accomplished during the GC reaction by inter- and intraclonal competition (18, 25, 47, 54). Nonetheless, several incongruent observations suggest that some affinity-driven selection, perhaps even most, takes place outside of the GC microenvironment.

First, affinity maturation of serum antibody continues long after the usual termination of primary GC responses. As early as 1972, Davie and Paul noted a 25-fold increase in the affinity of serum antibody ($K_a = 2.5 \times 10^7\ M^{-1}$ to $6.3 \times 10^8\ M^{-1}$) for the 2,4-dinitrophenyl hapten from day 45 to 171 of a primary response (38), well after the end of most primary GC reactions (53). Another incongruent observation is that mature GCs often contain B cell populations that express receptor affinities below that of the serum

antibody (55).[2] Splenic GCs support oligoclonal lymphocyte populations that show no evidence for significant B cell trafficking between GCs and thus no homogenization of selected populations (17). Although B cells in the same GC bear receptors with similar affinities, GCs in the same spleen can hold B cell populations with hapten-specific affinities that differ by 100-fold (55 and Shimoda, M., J. Dal Porto, and G. Kelsoe, unpublished observations). Finally, limited affinity maturation has been observed in lymphotoxin-α–deficient mice (37). Such mice are unable to form splenic GCs in response to noninflammatory antigens.

To determine the extent and role of post-GC selection in affinity maturation, we measured the affinity of hapten-specific AFCs and serum antibody over a period of 4 mo (119 d) after primary immunization with NP–CG. Increased numbers of BM AFCs were correlated with persistent titers of serum antibody (Fig. 1) and both AFCs (Fig. 3) and antibody (Fig. 4) exhibited coordinated increases in affinity for the NP hapten. This affinity maturation took place over the entire period of study, even after the end of the GC response in the spleen (Fig. 2).

The clonal selection responsible for increased affinity of serum antibody and BM AFCs in the post-GC phase was reflected in the somatic genetics of the BM AFC population (Table 2). In concert with late affinity maturation, cells bearing VDJ rearrangements characteristic of high affinity anti-NP antibody, e.g., using the V_HV186.2 and DFL16.1 gene segments and the YYGS motif in CDR3 (42, 48), accumulated in the BM AFC compartment. From day 46 to 119 of the response, the distribution of replacement mutations shifted dramatically from CDR2 to CDR1, without substantial increases in mutation frequencies. These changes in the BM AFC population are best explained by interclonal competition and selection after the GC reaction has ended. This sequence analysis (Table 2) also suggests that the GC reaction is the major, if not sole, source of V_H mutations present in BM AFCs. The rate of accumulation for V_H mutations in BM AFCs was greatest during the active GC reaction and the maximum frequency of mutations achieved in the BM AFC population, 4.6 per V_H gene segment, did not differ dramatically from that present in splenic GC B cells (3.8 per V_H gene segment) recovered by fluorescence-activated cell sorting at day 16 of the response (56). Late affinity maturation acts upon the genetic diversity generated early in the response; BM AFCs, perhaps even those that are unmutated, appear to be derived from GC B cells.

This notion is supported by our use of the MR1 antibody to define a cell compartment responsible for the generation of high affinity BM AFCs and serum antibody (Fig. 5). Administration of this CD154-specific antibody after day 6 of the response to NP–CG has no effect on early primary antibody titers (52), the generation of T cell help (57), or T cell memory as determined by in vitro recall response (data not shown). However, the MR1 antibody does abrogate the GC reaction within hours of its injection (52) without the induction of significant apoptosis in B cells (30, 58). The MR1-treatment used in this study completely eliminated all splenic GCs as determined by histology and the enumeration of GL-7^+ $B220^+$ splenocytes (data not shown); continuing surveys found no evidence for the re-formation of GCs. Administration of MR1 antibody after the end of the GC reaction had no discernable effect on NP-specific BM AFCs or serum antibody level (data not shown). Thus, the progenitors of high affinity BM AFCs and GC B cells share sensitivity to suppression by the MR1 antibody during the second and third weeks of the response.

Despite the complete loss of GCs and splenic B cells bearing the GC phenotype, affinity maturation was present in all mice treated with MR1 antibody. Indeed, although disruption of CD40–CD154 interactions lowered the frequency of high affinity BM AFCs and suppressed the average affinity of serum antibody, antigen-driven selection was equally efficient in MR1-treated and control mice (Fig. 6). Even the administration of MR1 antibody during the late phase (days 46–50) of the primary response did not suppress affinity maturation in the BM AFC compartment. These results demonstrate that clonal selection among BM AFCs is independent of the GC microenvironment and resistant to blockade of CD154-mediated costimulation.

In contrast to a similar study by Smith et al. (35), we did not observe an early plateau in the affinity of BM AFC. Nor did we observe preferential, early recruitment of AFCs carrying the affinity-enhancing W→L mutation at position 33 of the V186.2 V_H gene segment (35, 49); instead, a maximum of only one-fourth of V_HV186.2 rearrangements recovered from BM AFCs carried this exchange at days 46 and 119 after immunization (Table 2). These contradictions may be due to very different experimental approaches for the isolation of NP-binding B cells. Smith et al. determined the affinity and somatic genetics of BM AFCs only after antigen-based selection using a fluorescent NP-hapten (35), a process that may have biased the selected population for high affinity. Biased selection might be heightened in BM AFC populations, since surface Ig expression by these cells is low (23). Instead, we enriched NP-binding BM AFCs based on their expression of λ1 and CD138. Subsequently, cloned cDNAs were sequenced without further selection, such as colony hybridizations to detect CDR3 sequences typical of primary NP-specific B cells (49). Thus, although our selection criteria limited our study to $\lambda1^+$ cells and rearrangements of the V3 and V186.2 V_H subfamilies, antibody affinity and CDR3 diversity were unconstrained.

One might argue against the specificity of BM AFCs collected with regard to only λ1 and CD138 expression. However, we believe that the fraction of VDJ rearrangements amplified from nonspecific B cells was negligible, since nearly one-half of the selected cells secreted NP-binding IgG_1 antibody and the majority of amplified VDJ rearrangements contained the V186.2 gene segment despite the ability of our PCR primers to amplify many other related V_H gene segments (47, 49). Furthermore, we did not detect $\lambda1^+$ $CD138^+$ cells in BM after depletion of IgM^+ Mac-I^+ Gr-I^+ Thy1.2^+ cells from 8–20-wk-old naive mice (data not shown). Thus, we propose that the relatively low

frequency of the W→L mutation in our study does not reflect contamination by large numbers of nonspecific B cells but represents the true pattern of clonal selection in vivo without the confounding effects of artifactual enrichment.

In the primary response to NP–CG, affinity maturation of the serum antibody develops in two stages of clonal selection within and outside GCs. While GCs are present, antigen-driven selection progressed rapidly but could be halted by interrupting CD40–CD154 interactions with injections of the MR1 antibody. However, even after the GC reaction waned, affinity maturation and clonal selection continued, independent of GC structure and inhibition by MR1. Thus, the primary role for GCs in the affinity maturation of serum antibody seems to be the generation of high affinity variants by V(D)J hypermutation; afterwards, antigen-driven interclonal selection can occur outside of the GC microenvironment. Long-term clonal selection in the post-GC environment offers the opportunity to continue to improve the antigen-selected repertoire by allowing direct competition between the progeny of both high and lower affinity GC B cells. This process does not seem to take place between the isolated B cell populations present in different GCs, even when those populations are separated by only 20–50 μm (16).

The important question of where and how clonal selection takes place in the post-GC environment remains unanswered. The maintenance of memory B cells is thought to be dependent on the presence of persistent antigen (59) and ~10% of memory B cells are still in cell cycle at day 140 after primary immunization (60). These observations suggest that memory B cells are frequently restimulated by antigen held on follicular dendritic cells (11–13). One possible mechanism for continued selection might be competition among memory B cells for restimulation with persistent antigen. In support of this idea, it has been suggested that BM AFCs are generated by the migration of restimulated memory B cells from the spleen after secondary challenge (33, 61). In humans, B cells with memory phenotype have been shown to accumulate in BM with age, presumably as a consequence of a lifetime's exposure to antigens (62). If this were the case in mice, clonal selection in the BM AFCs might represent the transition of selected, memory cells into AFCs (20, 34, 61).

However, we do not believe that restimulation of memory cells accounts for affinity maturation late in the primary response. Recent labeling studies (23) demonstrate that the BM AFC compartment is not sustained by the proliferation of (memory) B lymphocytes but represents an independent, long-lived population. Furthermore, BM AFC numbers, affinity, and antibody production are not diminished by administration of the MR1 antibody after the primary GC reaction is complete. In contrast, secondary B cell responses are highly dependent on CD154-mediated costimulation as they are dramatically suppressed by MR1 antibody (57). Indeed, BM AFCs may directly compete for activation by antigen; unlike the early AFCs present in the spleen, BM AFCs express mIg and exhibit low levels of proliferation (23). However, the question still remains as to where the antigen depot required for this competitive stimulation might be located.

Although many studies have focused on memory B cells to examine the protective role of humoral immune responses, the AFCs in the BM compartment have been relatively neglected despite their significant contribution to the maintenance and quality of serum antibody (1, 20, 23, 35, 61). Recent accumulating data suggest that BM AFCs are a unique population distinct from the terminally differentiated AFCs present in secondary lymphoid tissues. Further studies are required to determine the contribution of these cells to protective immunity and to understand the biology of their selection and longevity.

We thank Dr. Toshitada Takemori and the members of his laboratory for their hospitality and support during the visit of Y. Takahashi.

This work was supported by in part by U.S. Public Health Service grants AI-24335, AG-10207, and AG-13789. Y. Takahashi is the recipient of a research fellowship from the Japan Society for the Promotion of Science for Young Scientists and G. Kelsoe received funds from the Jeanne M. and Joseph P. Sullivan Foundation and The Santa Fe Institute.

Address correspondence to Garnett Kelsoe, University of Maryland School of Medicine, 655 W. Baltimore St., Baltimore, MD 21201. Phone: 410-706-5927; Fax: 410-706-2129; E-mail: gkelsoe@umabnet.ab.umd.edu

Received for publication 17 November 1997 and in revised form 9 January 1998.

References

1. Ahmed, R., and D. Gray. 1996. Immunological memory and protective immunity: understanding their relation. *Science.* 272:54–60.

2. Simonsen, O., and K. Kjeldsen. 1984. Immunity against tetanus and effect of revaccination 25–30 years after primary vaccination. *Lancet.* 2:1240–1242.

3. Cohen, D., M.S. Green, E. Katzenelson, R. Slepon, H. Bercovier, and M. Wiener. 1994. Long-term persistence of anti-diphtheria toxin antibodies among adults in Israel. Implications for vaccine policy. *Eur. J. Epidemiol.* 10:267–270.
4. Eisen, H.N., and G.W. Siskind. 1964. Variations in affinities of antibodies during the immune response. *Biochemistry*. 3: 996–1008.
5. Siskind, G.W., and B. Benacerraf. 1969. Cell selection by antigen in the immune response. *Adv. Immunol.* 10:1–50.
6. Griffiths, G.M., C. Berek, M. Kaartinen, and C. Milstein. 1984. Somatic mutation and the maturation of the immune response. *Nature*. 312:271–275.
7. French, D.L., R. Laskov, and M.D. Scharff. 1989. The role of somatic hypermutation in the generation of antibody diversity. *Science*. 244:1152–1157.
8. Berek, C., G.M. Griffiths, and C. Milstein. 1985. Molecular events during maturation of the immune response to oxazolone. *Nature*. 316:412–418.
9. Cumano, A., and K. Rajewsky. 1986. Clonal recruitment and somatic mutation in the generation of immunological memory to the hapten NP. *EMBO (Eur. Mol. Biol. Organ.) J.* 5:2459–2468.
10. Foote, J., and C. Milstein. 1991. Kinetic maturation of an immune response. *Nature*. 352:530–532.
11. Nossal, G.J.V., G.L. Ada, and C.M. Austin. 1964. Antigens in immunity. IV. Cellular localization of ^{125}I and ^{131}I-labelled flagella in lymph nodes. *Aust. J. Exp. Biol. Med. Sci.* 42:311–330.
12. Tew, J.G., and T.E. Mandel. 1979. Prolonged antigen half-life in the lymphoid follicules of specifically immunized mice. *Immunology*. 37:69–76.
13. Mandel, T.E., T.E.R. Phipps, A. Abbot, and J.G. Tew. 1980. The follicular dendritic cell: long term antigen retention during immunity. *Immunol. Rev.* 53:29–59.
14. Gray, D. 1988. Recruitment of virgin B cells into an immune response is restricted to activation outside of lymphoid follicles. *Immunology*. 65:73–79.
15. Vonderheide, R.H., and S.V. Hunt. 1990. Immigration of thoracic duct B lymphocytes into established GC in the rat. *Eur. J. Immunol.* 20:79–86.
16. Jacob, J., R. Kassir, and G. Kelsoe. 1991. In situ studies of the primary immune response to (4-hydroxy-3-nitrophenyl)acetyl. I. The architecture and dynamics of responding cell populations. *J. Exp. Med.* 173:1165–1175.
17. Jacob, J., and G. Kelsoe. 1992. In situ studies of the primary immune response to (4-hydroxy-3-nitrophenyl)acetyl. II. A common clonal origin for PALS-associated foci and germinal centers. *J. Exp. Med.* 176:679–687.
18. McHeyzer-Williams, M.G., M.J. McLean, P.A. Lalor, and G.J.V. Nossal. 1993. Antigen-driven B cell differentiation in vivo. *J. Exp. Med.* 178:295–307.
19. Smith, K.G.C., T.D. Hewitson, G.J.V. Nossal, and D.M. Tarlinton. 1996. The phenotype and fate of the antibody-forming cells of the splenic foci. *Eur. J. Immunol.* 26:444–448.
20. Benner, R., W. Hijmans, and J.J. Haaijman. 1981. The bone marrow: the major source of serum immunoglobulins, but still a neglected site of antibody formation. *Clin. Exp. Immunol.* 46:1–8.
21. Slifka, M.K., M. Matloubian, and R. Ahmed. 1995. Bone marrow is a major site of long-term antibody production after acute viral infection. *J. Virol.* 69:1895–1902.
22. Vieira, P., and K. Rajewsky. 1988. The half-lives of serum immunoglobulins in adult mice. *Eur. J. Immunol.* 18:313–316.
23. Manz, R.A., A. Thiel, and A. Radbruch. 1997. Lifetime of plasma cells in the bone marrow. *Nature*. 388:133–134.
24. Jacob, J., G. Kelsoe, K. Rajewsky, and U. Weiss. 1991. Intraclonal generation of antibody mutants in germinal centers. *Nature*. 354:389–392.
25. Berek, C., A. Berger, and M. Apel. 1991. Maturation of the immune response in germinal centers. *Cell*. 67:1121–1129.
26. MacLennan, I.C.M. 1994. Germinal centers. *Annu. Rev. Immunol.* 12:117–139.
27. Kelsoe, G. 1996. Life and death in germinal centers (redux). *Immunity*. 4:107–111.
28. Pulendran, B., G. Kannourakis, S. Nouri, K.G.C. Smith, and G.J.V. Nossal. 1995. Soluble antigen can cause enhanced apoptosis of germinal-centre B cells. *Nature*. 375:331–334.
29. Shokat, K.M., and C.C. Goodnow. 1995. Antigen-induced B-cell death and elimination during germinal-centre immune responses. *Nature*. 375:334–338.
30. Han, S., B. Zheng, J. Dal Porto, and G. Kelsoe. 1995. In situ studies of the primary immune response to (4-hydroxy-3-nitrophenyl)acetyl. IV. Affinity-dependent, antigen-driven B cell apoptosis in germinal centers as a mechanism for maintaining self-tolerance. *J. Exp. Med.* 182:1635–1644.
31. Zheng, B., S. Han, Q. Zhu, R. Goldsby, and G. Kelsoe. 1996. Alternative pathways for the selection of antigen-specific peripheral T cells. *Nature*. 384:263–266.
32. Han, S., B. Zheng, D.G. Schatz, E. Spanopoulou, and G. Kelsoe. 1996. Neoteny in lymphocytes: Rag-1 and Rag-2 expression in germinal center B cells. *Science*. 274:2092–2094.
33. Koch, G., D.G. Osmond, M.H. Julius, and R. Benner. 1981. The mechanism of thymus-dependent antibody formation in bone marrow. *J. Immunol.* 126:1447–1451.
34. Dilosa, R.M., K. Maeda, A. Masuda, A. Szakal, and J.G. Tew. 1991. Germinal center B cells and antibody production in the bone marrow. *J. Immunol.* 146:4071–4077.
35. Smith, K.G.C., A. Light, G.J.V. Nossal, and D.M. Tarlinton. 1997. The extent of affinity maturation differs between the memory and antibody-forming cell compartments in the primary immune response. *EMBO (Eur. Mol. Biol. Organ.) J.* 16: 2996–3006.
36. Schroder, A.E., A. Greiner, C. Seyfert, and C. Berek. 1996. Differentiation of B cells in the nonlymphoid tissue of the synovial membrane of patients with rheumatoid arthritis. *Proc. Natl. Acad. Sci. USA*. 93:221–225.
37. Matsumoto, M., S.F. Lo, C.J.L. Carruthers, J. Min, S. Mariathasan, G. Huang, D.R. Plas, S.M. Martin, R.S. Geha, M.H. Nahm, and D.D. Chaplin. 1996. Affinity maturation without germinal centres in lymphotoxin-α–deficient mice. *Nature*. 382:462–466.
38. Davie, J.M., and W.E. Paul. 1972. Receptors on immunocompetent cells. V. Cellular correlates of the "Maturation" of the immune response. *J. Exp. Med.* 135:660–674.
39. Jack, R.S., T. Imanishi-Kari, and K. Rajewsky. 1977. Idiotypic analysis of the response of C57BL/6 mice to the (4-hydroxy-3-nitrophenyl)acetyl group. *Eur. J. Immunol.* 8:559–565.
40. Makela, O., and K. Karjalainen. 1977. Inherited immunoglobulin idiotypes of the mouse. *Immunol. Rev.* 34:119–138.
41. Bothwell, A.L.M., M. Paskind, M. Reth, T. Imanishi-Kari, K. Rajewsky, and D. Baltimore. 1981. Heavy chain variable region contribution to the NP^b family of antibodies: somatic mutation evident in a γ2a variable region. *Cell*. 24:625–637.
42. Cumano, A., and K. Rajewsky. 1985. Structure of primary anti-(4-hydroxy-3-nitrophenyl)acetyl (NP) antibodies in normal and idiotypically suppressed C57BL/6 mice. *Eur. J. Immu-*

nol. 15:512–520.
43. Herzenberg, L.A., S.J. Black, T. Tokuhisa, and L.A. Herzenberg. 1980. Memory B cells at successive stages of differentiation. Affinity maturation and the role of IgD receptors. *J. Exp. Med.* 151:1071–1087.
44. Jones, P.T., P.H. Dear, J. Foote, M.S. Neuberger, and G. Winter. 1986. Replacing the complementarity-determining regions in a human antibody with those from a mouse. *Nature*. 321:522–525.
45. Reth, M., T. Imanishi-kari, and K. Rajewsky. 1979. Analysis of the repertoire of anti-NP antibodies in C57BL/6 mice by cell fusion. II. Characterization of idiotopes by monoclonal anti-idiotope antibodies. *Eur. J. Immunol.* 9:1004–1013.
46. Gu, H., D. Tarlinton, W. Müller, K. Rajewsky, and I. Förster. 1991. Most peripheral B cells in mice are ligand selected. *J. Exp. Med.* 173:1357–1371.
47. Jacob, J., J. Przylepa, C. Miller, and G. Kelsoe. 1993. In situ studies of the primary immune response to (4-hydroxy-3-nitrophenyl)acetyl. III. The kinetics of V region mutation and selection in germinal center B cells. *J. Exp. Med.* 178: 1293–1307.
48. Blier, P.R., and A. Bothwell. 1987. A limited number of B cell lineages generates the heterogeneity of a secondary immune response. *J. Immunol.* 139:3996–4006.
49. Weiss, U., and K. Rajewsky. 1990. The repertoire of somatic antibody mutants accumulating in the memory compartment after primary immunization is restricted through affinity maturation and mirrors that expressed in the secondary response. *J. Exp. Med.* 172:1681–1689.
50. Tao, W., F. Hardardottir, and A.L.M. Bothwell. 1993. Extensive somatic mutation in the Ig heavy chain V genes in a late primary anti-hapten immune response. *Mol. Immunol.* 30: 593–602.
51. Noelle, R.J., M. Roy, D.M. Shepherd, I. Stamenkovic, J.A. Ledbetter, and A. Aruffo. 1992. A 39-kDa protein on activated helper T cells binds CD40 and transduces the signal for cognate activation of B cells. *Proc. Natl. Acad. Sci. USA*. 89: 6550–6554.
52. Han, S., K. Hathcock, B. Zheng, T.B. Kepler, R. Hodes, and G. Kelsoe. 1995. Cellular interaction in germinal centers. Roles of CD40 ligand and B7-2 in established germinal centers. *J. Immunol.* 155:556–567.
53. Liu, Y.-J., J. Zhang, P.J.L. Lane, E.Y.-T. Chan, and I.C.M. MacLennan. 1991. Sites of specific B cell activation in primary and secondary responses to T cell–dependent and T cell–independent antigens. *Eur. J. Immunol.* 21:2951–2962.
54. Weiss, U., R. Zoebelein, and K. Rajewsky. 1992. Accumulation of somatic mutants in the B cell compartment after primary immunization with a T cell–dependent antigen. *Eur. J. Immunol.* 22:511–517.
55. Vora, K.A., and T. Manser. 1995. Altering the antibody repertoire via transgene homologous recombination: evidence for global and clone-autonomous regulation of antigen-driven B cell differentiation. *J. Exp. Med.* 181:271–281.
56. Han, S., S.R. Dillon, B. Zheng, M. Shimoda, M.S. Schlissel, and G. Kelsoe. V(D)J recombinase activity in a subset of germinal center B lymphocytes. *Science.* 278:301–305.
57. Foy, T.M., D.M. Shepherd, F.H. Durie, A. Aruffo, J.A. Ledbetter, and R.J. Noelle. 1993. In vivo CD40–gp39 interactions are essential for thymus dependent humoral immunity. II. Prolonged suppression of the humoral immune response by an antibody to the ligand for CD40, gp39. *J. Exp. Med.* 178:1567–1575.
58. Foy, T.M., A. Aruffo, J. Bajorath, J.E. Buhlmann, and R.J. Nolle. 1996. Immune regulation by CD40 and its ligand gp39. *Annu. Rev. Immunol.* 14:591–617.
59. Gray, D., and H. Skarvall. 1988. B-cell memory is short-lived in the absence of antigen. *Nature.* 336:70–73.
60. Schittek, B., and K. Rajewsky. 1990. Maintenance of B-cell memory by long-lived cells generated from proliferating precursors. *Nature.* 346:749–751.
61. Benner, R., A. Van Oudenaren, and H. De Ruiter. 1977. Antibody formation in mouse bone marrow. IX. Peripheral lymphoid organs are involved in the initiation of bone marrow antibody formation. *Cell. Immunol.* 34:125–137.
62. Paramithiotis, E., and M. Cooper. 1997. Memory B lymphocytes migrate to the bone marrow in humans. *Proc. Natl. Acad. Sci. USA*. 94:208–212.